



ELSEVIER

Available online at www.sciencedirect.com

SCIENCE @ DIRECT®

Nuclear Instruments and Methods in Physics Research A 542 (2005) 376–382

NUCLEAR
INSTRUMENTS
& METHODS
IN PHYSICS
RESEARCH
Section A

www.elsevier.com/locate/nima

Discrete tomography in neutron radiography

Attila Kuba^{a,*}, Lajos Rodek^a, Zoltán Kiss^a, László Ruskó^a,
Antal Nagy^a, Márton Balaskó^b

^aDepartment of Image Processing and Computer Graphics, University of Szeged, Árpád tér 2, H-6720 Szeged, Hungary

^bKFKI Atomic Energy Research Institute, Konkoly Thege út Budapest, Hungary

Available online 2 March 2005

Abstract

Discrete tomography (DT) is an imaging technique for reconstructing discrete images from their projections using the knowledge that the object to be reconstructed contains only a few homogeneous materials characterized by known discrete absorption values. One of the main reasons for applying DT is that we will hopefully require relatively few projections. Using discreteness and some a priori information (such as an approximate shape of the object) we can apply two DT methods in neutron imaging by reducing the problem to an optimization task. The first method is a special one because it is only suitable if the object is composed of cylinders and sphere shapes. The second method is a general one in the sense that it can be used for reconstructing objects of any shape. Software was developed and physical experiments performed in order to investigate the effects of several reconstruction parameters: the number of projections, noise levels, and complexity of the object to be reconstructed. We give a summary of the experimental results and make a comparison of the results obtained using a classical reconstruction technique (FBP). The programs we developed are available in our DT reconstruction program package DIRECT.

© 2005 Elsevier B.V. All rights reserved.

PACS: 07.85.Fm; 87.59.Hp

Keywords: Discrete tomography; Radiography; Parameterized reconstruction; Statistical relaxation

1. Introduction

Discrete tomography (DT) is a special imaging technique for determining the cross-sections of objects from their projections. It may be applied if

the object to be reconstructed consists of a small number of homogeneous regions with known absorption coefficients. For example, if the object is made of pure iron, the number of regions is two (iron and air) and the reconstructed function can only take two values: the absorption coefficient for the iron and for the air. With DT we make use of the fact that the function has a known discrete range. This is the key difference between DT

*Corresponding author. Tel.: +36 62 546 396;
fax: +36 62 546 397.

E-mail address: kuba@inf.u-szeged.hu (A. Kuba).

techniques and the classical reconstruction techniques, where the function/object can have arbitrary (non-negative) values. A knowledge of the discrete absorption values may allow us to use DT methods to reconstruct such objects from a relatively few number of projections (e.g. 2–4) and/or improve the quality of the reconstruction (for a summary of DT see Ref. [1]).

2. Preprocessing

The input images of the reconstruction process are the projection images of the object taken from different directions. In order to get an approximation of the line integrals of the object along transmitting rays, we first have to transform the detected intensities as follows:

$$\log \frac{I_0}{I} = \int_{\ell} \mu(x, y) du$$

where $\mu(x, y)$ denotes the attenuation coefficient of the object at point (x, y) , while I_0 and I are the initial and detected intensities of the transmission rays. After this logarithmic transformation the necessary line integrals are available for the remaining steps and the reconstruction.

If the projections are images produced by neutron rays, then the images are distorted owing to several effects. Some of the *distortions are due to the properties of the image acquisition system*. For example, the detector system is not uniformly sensitive in the whole field of view. Another problem can be if the intensity of the rays or the sensitivity of the camera changes during the acquisition time. If the projections are not taken exactly according to the necessary positions (motion, incorrect settings), the input data again need to be corrected. Furthermore, in our experience it was often the case that the images also contained white specks that had to be removed. Additional distortions can be modeled by supposing some level of noise in the image.

In order to reduce the effects of these distortions we implemented several correction methods—so-called *preprocessing* steps—in our system before carrying out any kind of reconstruction.

1. *Cropping* the relevant area from the projection images which contains the object. This step is very useful if the size of the projection image is big and the projections of the object cover only a small part of the whole field of view.
2. *Registration*. If the projection of the axis of rotation does not cover the vertical centerline in the images it will cause a serious problem. In the simplest case (i.e. when the projections are simply translated), this effect can be corrected by translating the projections along a suitable sine curve. If a rotation and translation of the projections are also possible during the acquisition, then some *rigid registration* may be required, which is applicable only if the object fulfils certain symmetry conditions.
3. *Intensity correction*. If the sensitivity of the imaging system varies during the acquisition the images should be corrected such that the average intensity in the background area is roughly constant.
4. *Uniformity correction* can be performed if an “empty” reference image is available which does not contain the projection of the object.
 - 4.1. For each pixel in each projection let $H_j = I/B_j$, where B_j is the intensity level of the j th pixel on the reference image.
 - 4.2. The pixel intensities for each projection are scaled up/down by the corresponding H_j factor.
5. In those cases where there was a large amount of noise, we applied *thresholded median filter*. The pixel intensities in each projection are replaced by $\text{med}(N(j))$ if $\text{med}(N(j)) \geq \text{thr}$, where $\text{med}(N(j))$ denotes the median of the pixel values in some neighborhood of pixel j and thr is a feasible threshold.

The effects of the correction steps can be seen in Fig. 1. Since the object covers only a small portion of the projection images, the relevant area from each image is cropped (Fig. 1b, first column). Afterwards intensity and uniformity corrections are performed followed by the registration step. For the results of these three consecutive steps, see Fig. 1b, first row.

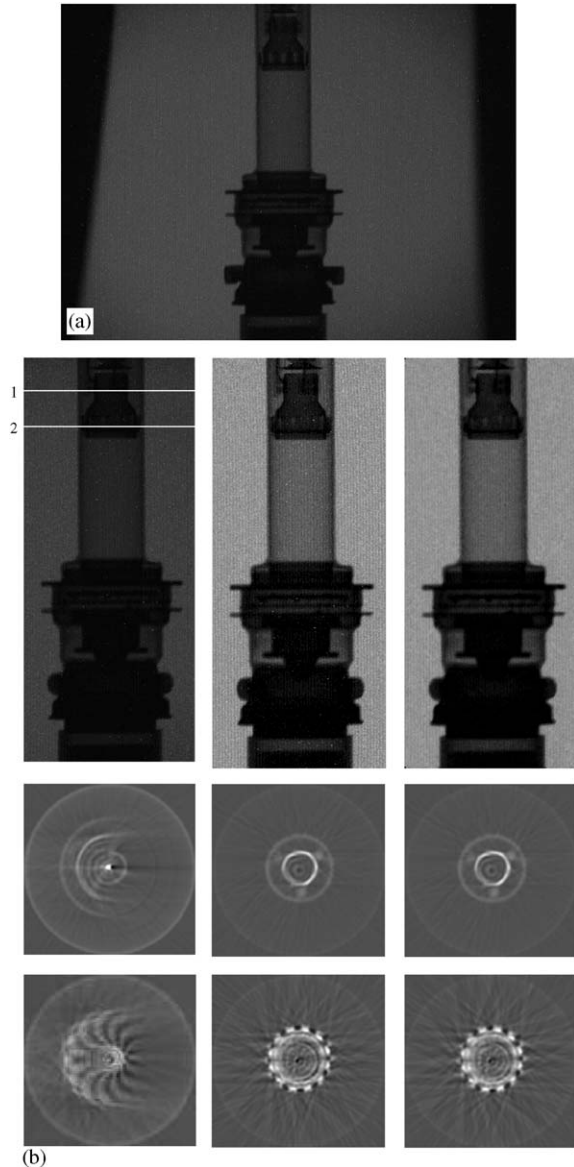


Fig. 1. The effects of the correction steps using the projection images of a Vidicon tube. (a) One of the original projection images. (b) First column: Images after cropping. Second column: Images after correction step 4. Third column: Images after correction step 5. First row: Projection images. Second row: Reconstructed cross-sections indicated by line 1. Third row: Reconstructed cross-sections indicated by line 2.

3. Discrete tomographic reconstruction methods

Briefly, the essence of our reconstruction methods is to minimize the following $\Phi(F)$ objective

functional:

$$\Phi(F) = \sum_{\vartheta} \|\text{proj}(F, \vartheta) - p_{\vartheta}\|^2 + \gamma \|F - F_0\|^2$$

where p_{ϑ} denotes the input projection obtained at angle ϑ , F is the image function approximating the solution during iterations, $\text{proj}(F, \vartheta)$ denotes the projection of the image F taken at angle ϑ , and γ is the so-called relaxation parameter. The projections need not have a constant angular distance; they can be taken from an arbitrary set of angles.

The first term expresses how far the projections of the actual F are from the given projection data p_{ϑ} , while the second term describes the difference between the actual F and a given prototype object F_0 . That is, the second term includes the a priori information that the object to be reconstructed is similar to another object F_0 . If the object F_0 is the zero image, then the second term says that we are interested in a solution that has a small norm $\|F\|^2$. The relaxation parameter γ is needed to determine the relative weight between the first and second terms. A big γ can yield solutions that are more similar to the prototype F_0 and less suitable for the given projection data.

We developed two reconstruction methods, based on previous work [5,6]. The first is a pixel-based method and the second is a kind of parameterized object reconstruction. Both methods reduce the reconstruction to the optimization problem mentioned above, which may be solved by using simulated annealing [2]. Since simulated annealing is a statistical iterative optimization approach, the result will be achieved through a sequence of approximating images, where the $(n+1)$ th image is constructed by modifying the n th image according to a given *rule*. The two reconstruction methods essentially differ in the representation of the object F . Both techniques were integrated into the system called DIRECT [3], which is a framework for a collection of DT methods being developed at our department.

3.1. Pixel-based reconstruction

In this case, the object F is represented as a digital image. If the object is homogeneous, then the pixels can take only two possible values,

namely attenuation coefficients of the background and object picture elements (in many cases they can be 0 and 1 if we have binary images).

With binary images the rule for changing the image F is quite simple. Let us randomly take a pixel of F and change the 0 or 1 intensities to the other intensity value. In this way we get a new binary image F' that is different from F only in one pixel. If $\Phi(F') < \Phi(F)$ then we accept this change and we continue the iteration with the new image F' . Otherwise, image F' is still accepted with a probability p , or rejected with probability $(1-p)$, where p decreases during the iterations.

In general, if we have more than two materials in the object to be reconstructed, the pixel values are based on the given set of known attenuation coefficients of these materials, giving so-called *multilevel images*.

With multilevel images where F can take its values from the given known set $\{\mu_1, \mu_2, \dots, \mu_d\}$, the rule is different from the rule used for binary images. If F has values μ_i in the randomly selected position, the value of F' will be μ_{i-1} or μ_{i+1} .

Our DT system allows us to simulate *parallel* and *fan-beam projections* as well. In the first case it is assumed that the transmitting rays are strips with a given thickness and the detectors measure the total intensities in the strips. The rays of the fan-beam projections are emitted from a point source and the total transmitted intensities in the fan-shaped area between the source and detectors are computed.

3.2. Parameterized object reconstruction

Here it is supposed that the object to be reconstructed can be mathematically represented by some parametric functions. One example is when the object is just the combination of simple geometrical shapes like spheres, tubes and cylinders. Such a priori knowledge may greatly improve the quality of the reconstructed image.

Our second reconstruction method assumes that the object to be reconstructed consists of a tube encompassing a solid cylinder called the interior, which contains a known number of disjoint solid spheres or cylinders. It may be suitable for modeling pipelines, ball-bearings, and so on. In

addition, the object components can be made of up to four different substances. These are:

1. the tube;
2. the interior encompassed by the tube;
3. the spheres and cylinders contained in the interior;
4. and the background, which is usually air or vacuum.

Every sphere is uniquely determined by its radius and the coordinates of its center, which are the parameters of the sphere. Cylinders and tubes can be parameterized in a similar way. Objects like these can be described by the set of parameters called the configuration.

It should be noted here that the cross-sections of such objects consist of an annulus and several discs, all of which can be parameterized in a straightforward way.

The optimization of the functional $\Phi(F)$ is performed in the parameter space. The optimum is achieved by the following iterative algorithm. The procedure starts by building an initial configuration. At each iteration step, a new configuration is built by modifying one of the parameters of the current configuration. Invalid configurations, where the spheres are not in the interior, or spheres that are not disjoint but overlapping, are always rejected. If $\Phi(F') < \Phi(F)$ then $\Phi(F')$ becomes the current approximation. Otherwise, it may be accepted or rejected in the same way as in the pixel-based reconstruction method.

4. Simulation studies

The effectiveness of both pixel-based and parameterized object reconstruction methods was investigated on several phantoms containing circular cross-sections (Fig. 2, first column).

We studied the effect of noise on the reconstruction results of the two techniques. In each case 0% or 10% or 40% of noise was added to the projections before performing the reconstruction. In Fig. 2 it is readily seen that an increase in noise degrades the quality of the resultant cross-sections.

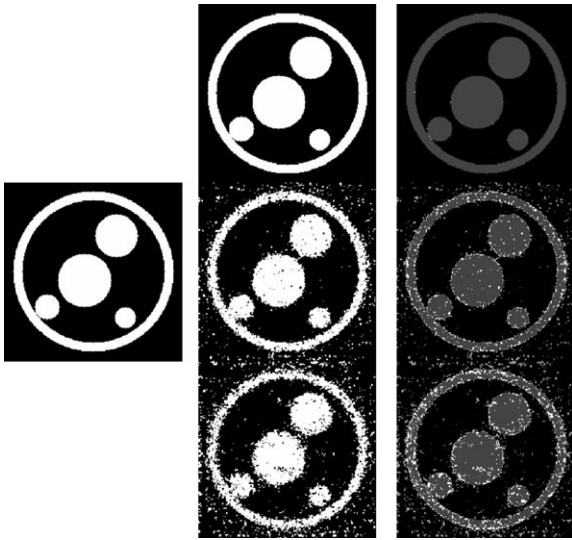


Fig. 2. The reconstruction of circles by the pixel-based method from exact and noisy projections (16 projections and 200 measurements/projection). First column: original object. First row: reconstructed object and the difference between the reconstructed and original images. Further rows: reconstruction from noisy projections (10% and 40% noise), reconstructed object and the difference between the reconstructed and original images.

However, the parameterized object reconstruction method shows high robustness even in the case of 40% noise, as shown in Fig. 3. As a matter of fact, even using noiseless projections did not yield notably better results.

We also analyzed how the number of projections used influenced the results (Fig. 4). Decreasing the number of projections to 12, the pixel-based method still gives quite good results, but a reconstruction from 10 or fewer projections shows an increasingly marked discrepancy between the original and the reconstructed object (Fig. 4, third column).

It is remarkable that the parameterized object reconstruction is only slightly biased on the number of used projections. As depicted in Fig. 5, it is usually sufficient to use only two projections for simpler objects (e.g. four circles or spheres). The algorithm itself is more sensitive to geometrical complexity (Fig. 5, third row).

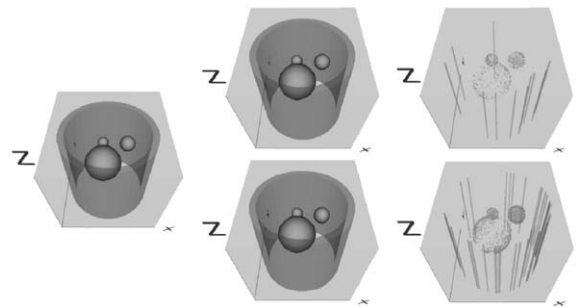


Fig. 3. The reconstruction of three spheres by the parametric method from noisy projections by VRML visualization (two projections and 100×100 measurements/projection). First column: original object. Second column: reconstructed object. Third column: difference between the reconstructed and original models. First and second rows: reconstruction in the presence of 10% and 40% noise, respectively.

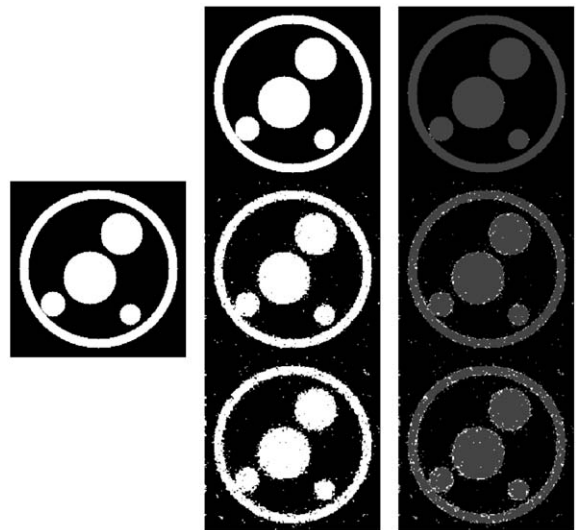


Fig. 4. The reconstruction of circles via the pixel-based method obtained from a different number of projections (0% noise, 200 measurements/projection). First column: original object. First row: reconstructed object from 12 projections and the difference between the reconstructed and original images. Further rows: reconstruction from 10 and eight projections, the reconstructed object and the difference between the reconstructed and original images.

5. Experiments

We had the opportunity to test the methods using real measurement data (Fig. 6a). In order to

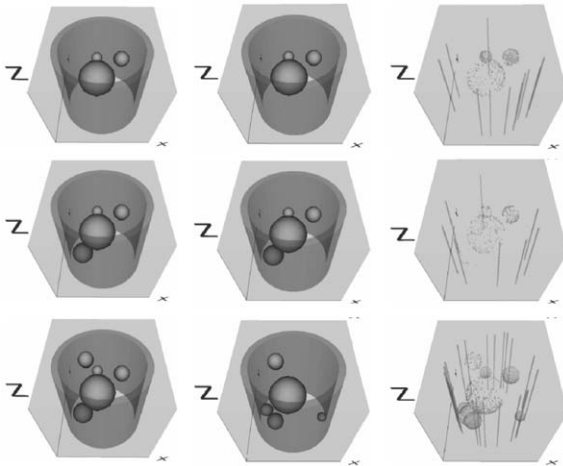


Fig. 5. Reconstruction using an increasing number of spheres by the parametric method via VRML visualization (10% noise, two projections, and 100×100 measurements/projection). First column: original object. Second column: reconstructed object. Third column: difference between the reconstructed and original models.

prove their efficiency we compared the results with those that were obtained by the classical FBP method, performed using SNARK93 [4]. (For further details about the object investigated, see Ref. [7].)

In Fig. 6 comparison of the results of FBP and pixel-based methods is presented. The cross-section denoted by 1 in Fig. 6b contains only two kinds of materials and, as was expected, the pixel-based method produced a good result (Fig. 6c). It is curious that the cross-section originally contained only three holes, but in Figs. 6b and c a fourth unexpected hole turned up in the center (due to homogeneity problems of the imaging system). This phenomenon did not arise when applying the parameterized algorithm (Fig. 7), due to the fixed number of cylinders.

We also tried the pixel-based approach on certain cross-sections (denoted by 2 in Fig. 6a) that contained three materials and even in this case it yielded an acceptable result.

In future research we plan to make improvements to the pixel-based technique to make it work more accurately on cross-sections consisting of

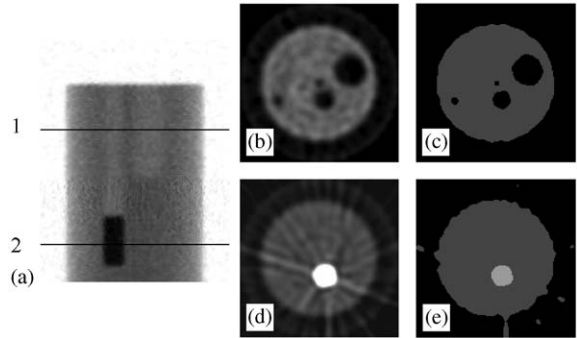


Fig. 6. The reconstruction of a solid cylinder with cylindrical holes. (a) One of the projections of the object. Two horizontal lines denoted by 1 and 2 indicate the positions of the selected cross-sections. (b) Cross-section 1 reconstructed by the classical method FBP. (c) Cross-section 1 reconstructed by the pixel-based DT method. (d) Cross-section 2 reconstructed by the classical method FBP. (e) Cross-section 2 reconstructed by the pixel-based DT approach.

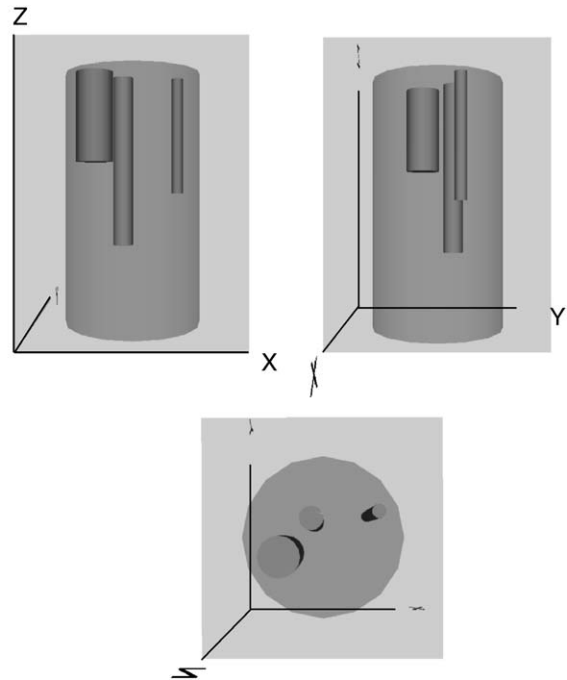


Fig. 7. Different views of the reconstructed object shown in Fig. 6. Images created by the parametric method (VRML visualization).

more than two materials, to reduce the noise sensitivity, and to reduce the number of necessary projections.

Acknowledgements

This work was supported by the NSF grant DMS 0306215 (Aspects of Discrete Tomography).

References

- [1] G.T. Herman, A. Kuba (Eds.), *Discrete Tomography. Foundations, Algorithms, and Applications*, Birkhäuser, Boston, 1999.
- [2] N. Metropolis, A.W. Rosenbluth, M.N. Rosenbluth, A.H. Teller, E. Teller, *J. Chem. Phys.* 21 (1953) 1087.
- [3] Homepage of DIRECT framework: <http://www.inf.u-szeged.hu/~direct/>
- [4] Homepage of SNARK93: <http://www.cs.gc.cuny.edu/~gherman/snark2001.html>
- [5] A. Kuba, L. Ruskó, L. Rodek, Z. Kiss, Preliminary results of discrete tomography in neutron imaging, *IEEE Trans. Nucl. Sci.*, submitted.
- [6] A. Kuba, L. Ruskó, L. Rodek, Z. Kiss, Application of discrete tomography in neutron imaging, in: *Proceedings of the Seventh World Conference on Neutron Radiography*, Rome, 2002, to be published.
- [7] Márton Balaskó, Attila Kuba, Antal Nagy, Zoltán Kiss, Lajos Rodek, László Ruskó, Neutron- gamma- and X-ray three-dimensional computer tomography at the Budapest research reactor, *Proceedings of the ITMNR* (2004) 140.